Thermal aging of power module assemblies based on ceramic heat sink and multilayers pressureless silver sintering

N. Botter, R. Khazaka, Y. Avenas, J.M. Missiaen, D. Bouvard, S. Azzopardi

Thermal aging of power module assemblies based on ceramic heat sink and multilayers pressureless silver sintering

N. Botter[a,b,c]*, R. Khazaka[a]*, Y. Avenas[b], J.M. Missiaen[c], D. Bouvard[c], S. Azzopardi[a]

[a]*Safran SA, Safran Tech, 1 rue des jeunes bois, Châteaufort, CS 80112, 78772 Magny-les-Hameaux, France*
[b]*Univ. Grenoble Alpes, CNRS, Grenoble INP, G2Elab, 38000 Grenoble, France*
[c]*Univ. Grenoble Alpes, CNRS, Grenoble INP, SIMAP, 38000 Grenoble, France*

Abstract

An assembly based on the deposition and pressureless sintering of successive silver layers on an Aluminum Nitride heat sink is studied in this paper. Sintered silver layers act as die attach, current tracks and adhesion layer on the ceramic. Compared to previous studies where silver sintering is only used as die attach, an additional degree of freedom on the sintering temperature of the ceramic adhesion and track layers is obtained. This allows the investigation of silver sintering at non-conventional temperatures (>400°C). The presented assembly is expected to endure high operating temperature since all its constituent materials are able to withstand such temperatures. The porosity of the sintered layer is controlled by the dwell time and the sintering temperature, and porosity values between 19% and 41% are obtained. The electrical and thermal conductivities of sintered layers as functions of joint porosity are in good agreement with the literature data and the assembly presents good mechanical properties with a shear strength value higher than 18 MPa. The assembly shows a high robustness during thermal storage at 200°C for 1000h. The microstructure and the electrical conductivity of track layers are both stable during the whole aging period. However, a slight improvement of the thermal response and the mechanical properties of the assembly is detected after 200h of aging followed by a stabilization until the end of the aging tests (1000h). Such observation is correlated to the microstructure coarsening of the sintered silver under the device and it is shown that this evolution is favored by the presence of the device.

1. Introduction

Aircraft manufacturers are expecting an increase of electrical power on-board in airplanes from 1MW to 10MW in 30 years. In order to achieve mass and volume gain, an increasing interest in using high density integrated power electronics modules in harsh environment has emerged. This trend is mainly pushed by the market introduction of high temperature wide band-gap Silicon Carbide (SiC) or Gallium Nitride (GaN) power semiconductor devices with junction temperature exceeding 200°C [1][2]. Therefore, robust packaging with high performance cooling systems are needed to insure the operation capability of electronic systems.

Conventional power modules are made by stacking several materials including semiconductors, solder alloys, metallized substrate, heat spreader and thermal interface material (Figure 1a). This assembly presents thermomechanical and thermal reliability issues in harsh environments. From the thermo-mechanical point of view, the Coefficient of Thermal Expansion (CTE) mismatch between the materials leads to high stresses during the lifetime of the power module. For instance, during large amplitude thermal cycling (300°C), it has been highlighted that 20 to 30 cycles are typically needed to crack or spall the Direct Bonded Copper (DBC) metalized substrate with Al_2O_3 or AlN ceramics [3]. The use of Si_3N_4 ceramics with copper bonded by Active Metal Brazing (AMB) technology improves the substrate reliability [4][5]. Since the Si_3N_4 thermal conductivity is half of the AlN one, thin ceramic is used in most cases (<300µm) and the warpage of the substrate becomes a serious issue.

Otherwise, the large soldered area between the substrate and the heat spreader has been identified as the most prominent failure risk which reduces the lifetime of the power modules and cracks appear after 3000 cycles with a temperature swing of 190°C [6]. On the other hand, during thermal storage above 150°C, brittle intermetallic compounds can be formed between the substrate metallization and the solder which affect the joint reliability [7]. In addition, organic Thermal Interface Materials (TIM)

*Corresponding author. nicolas.botter@grenoble-inp.fr / rabih.khazaka@safrangroup.com
Tel: +33 (0)6 48 89 39 95

like thermal greases, elastomers or phase changing films show limited stability at high temperatures and suffer from low thermal conductivity [8].

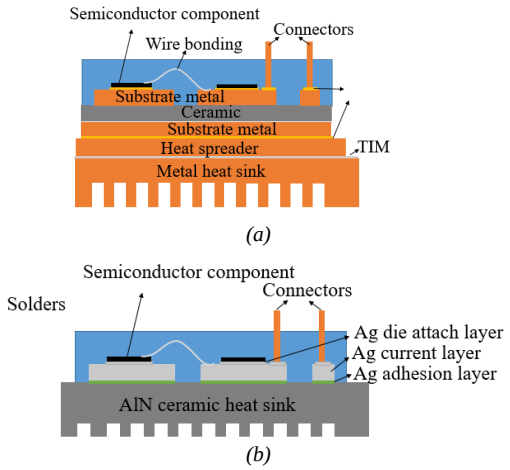

Figure 1: Schematic cross section of conventional power module assembly (a) and the one proposed in this paper (b).

Silver sintering has demonstrated its potential as an alternative to solders for high temperature applications and is compliant with regulation of the Restriction of Hazardous Substances (RoHS) [9]. However, for pressureless sintered joints, it was shown that the storage at high temperature (above 250°C) leads to an evolution of the porous joint microstructure while no modification of the microstructure has been observed at temperature below 150°C [10][11]. A mechanism of coarsening was revealed wherein oxygen plays a more important role than the traditional Ag thermal self-diffusion.

The aim of this paper is to evaluate the initial properties as well as their variations during high temperature thermal storage of an innovative assembly based on the use of pressureless sintered silver layers (with monitored densities) between an AlN heat sink and the semiconductor devices (Figure 2a). Consecutive sintered silver layers act as adhesion layer on the AlN ceramic, current track and die attach. It is expected that the package allows improving the module reliability thanks to the unique silver joint with no brittle intermetallic creation and the close coefficients of thermal expansion between the AlN and Si and the porous joint that can act as a buffer layer. In a more detailed fashion, the main technical contributions presented in this paper are listed hereafter:

1. The investigation of the properties of pressureless silver sintered track layers at unusual high temperatures (not compatible for die attach).
2. The mechanical properties at initial time and during high temperature isothermal aging of assemblies realized by using multiple sintered layer between an AlN ceramic and Si device.
3. The impact of long period isothermal aging on the microstructure, electrical and thermal properties of assemblies realized with multilayer silver sintered. Since silver sintered layers are used for track layer and die attach layer, the impact of the mechanical stresses induced by the device presence on the microstructure of the sintered joint will be highlighted.

2. Experiments

2.1. Samples preparation

For microstructural and electrical tests, a silver ink used as an adhesion layer was screen printed on the AlN plate using a 325-mesh stainless steel screen with an emulsion of 20 µm and then sintered at 850°C for 10 min in ambient air. The final thickness of the silver adhesion layer was about 7 µm after sintering. Once this step was completed, silver paste was screen printed on the adhesion layer by using a 100 µm thick stainless stencil. In order to achieve various densities, four sintering profiles were used (325°C-10 min, 400°C-10 min, 400°C-1 hour and 500°C-1 hour).

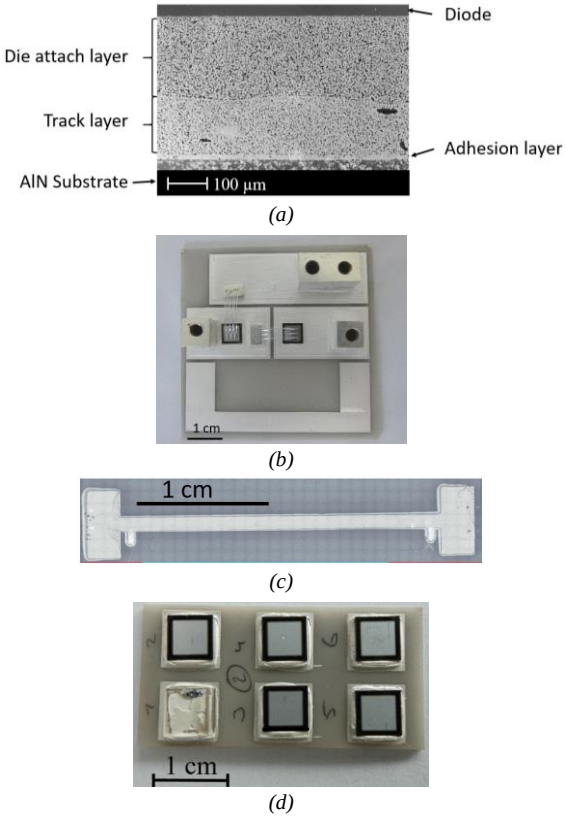

Figure 2: Cross-section of proposed assembly (a); sample used for transient thermal evaluation (b); sample used for electrical conductivity measurement (c); sample used for shear resistance measurement (d).

For transient thermal and mechanical tests, diode chips of 6×6 mm² with Ti/Ni/Ag backside metallization layers provided by ABB (5SLY12E1200) were used in the assembly. Thus, the samples were made of three different layers: the adhesion layer was achieved on the ceramic as described previously, the track layer was sintered at intermediate temperatures (500°C-1h or 400°C-10 min). Finally, the third silver paste layer used as die attach was sintered at lower temperature and reduced time (325°C-10 min) in order to avoid the degradation of the semiconductor device. The latter sintering profile corresponds to the maximum duration at the maximum temperature recommended for several semiconductor components. In addition, in a previous paper [12] the authors have investigated the sintering kinetics at 325°C. It has been found that the shrinkage rate was drastically reduced after 10 min at 325°C. Both second and third layers were printed using a 200 µm thick stainless stencil. A cross section of the proposed assembly is presented in Figure 2a. The samples used for transient thermal, electrical and shear resistance characterizations can be seen in Figure 2b, 2c and 2d respectively.

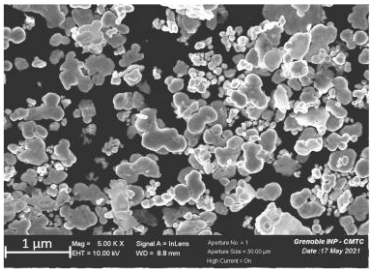

(a)

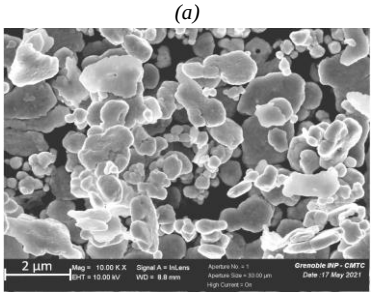

(b)

Figure 3: SEM views of debinded silver paste at magnification ×5000 (a) and ×10000 (b).

The silver paste used for this work is composed of micron sized silver particles. Scanning Electron Microscopy (SEM) top view of debinded silver paste is presented in Figure 3a and 3b. Dispersion in size of the particles is ranging between hundreds of nanometers and a few micrometers.

2.2. Tests setup

The electrical conductivity was measured at room temperature using the Kelvin measurement method for various sintering profiles. The thermal conductivity was deduced with the Wiedemann-Franz law.

The microstructure of sintered silver was investigated by SEM and Focused Ion Beam (FIB). The relative density (d) of the sintered joint was deduced from the measurement of volume and mass of a parallipipedic shape sample of sintered silver paste, with the weight density of pure silver as the reference, and the porosity (p) was calculated as 1 - d. The volume was defined by measuring the dimension of the sample with an optical microscope. In order to reduce the error on the porosity value, this measurement was performed on 3 different samples for each sintering condition.

Transient thermal measurements were achieved on the diodes after the injection of a current pulse of 120 A during 30 ms in order to limit the increase of die temperature to 100°C. The forward voltage drop V_f of the diodes for a current of 11.93 mA was used as an electrical thermosensitive parameter that allowed, once calibrated, the estimation of the junction temperature T_j during cooling. The calibration of the thermosensitive coefficient was performed by placing the samples inside an oven while measuring the threshold voltage V_f of the diode at different temperatures (Figure 4).

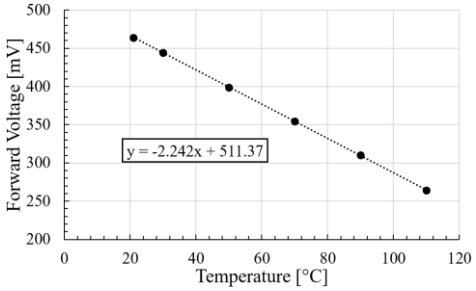

Figure 4: Calibration curve for thermal transient measurement showing the forward voltage vs the temperature.

The shear tests were carried out using a Royce 600 series bond test equipment with a head tool length of 8 mm (larger than the device length). The head tool was positioned 20 µm above the ceramic surface and the displacement rate was fixed at 1mm/min. The applied force is measured during the test until the failure detection. The shear stress was calculated by dividing the maximum measured force by the device area. For thermal and mechanical tests, at least 4 samples have been characterized for each condition to obtain acceptable statistics and to evaluate the measurements repeatability. Assemblies were aged in an oven at 200°C in air and were tested at different times during the aging with destructive and non-destructive tests. For non-destructive tests the same samples was characterized at various times

along the thermal storage.

3. Results and discussions

3.1. Initial properties

The porosity of the sintered layers for different maximum process temperatures and dwell times are presented in Table 1. The higher the temperature and the longer the sintering time, the lower the porosity. This is due to the fact that sintering is governed by thermally-activated diffusion phenomena. The minimal porosity has been found to be 19%.

T max *Dwell time*	*325°C* *10 min*	*400°C* *10 min*	*400°C* *1 h*	*500°C* *1 h*
Porosity rate [%]	*44*	*34*	*26*	*19*

Table 1: Porosity value for different thermal profiles.

The impact of porosity on the electrical and thermal conductivities is illustrated in Figure 5. The thermal conductivity was determined from electrical resistivity measurements and the application of the Wiedemann-Franz law. Results show that the lower the porosity of the sintered joint, the higher the electrical and thermal conductivity values. For the highest joint porosity obtained after sintering at 325°C for 10 min, an electrical conductivity of 1/3 of the bulk silver was measured corresponding to a thermal conductivity of 150 $W.m^{-1}.K^{-1}$. The obtained data are in good accordance with literature results obtained after pressure assisted silver sintering [13] and they will be very useful for the design of a power module with specified current rating and thermal resistance.

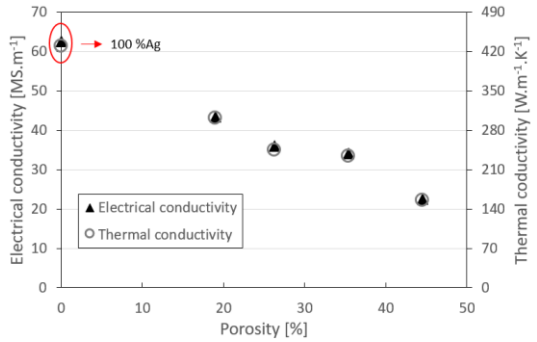

Figure 5: Electrical and thermal conductivities as functions of porosity.

The mechanical properties of the samples with Si diodes sintered at 325°C for 10 min on a second layer sintered at 500°C for 1 h or at 400°C for 10 min were evaluated. The mean value of shear stress was found to be 18 MPa and 21 MPa when the second layer is sintered at 400°C and 500°C, respectively. In both cases, the fracture takes place at the interfaces between the layer sintered at 325°C for 10 min and the device or the second layer (sintered at 400°C or 500°C) for all samples. Results on fracture analysis will be presented and discussed in section 3.2.

3.2. Thermal storage at 200°C

Sintering is governed by atomic diffusion. Diffusion phenomena are activated by temperature, and could occur during the lifetime of the power converter. The impact of aging at 200°C on the microstructure was first investigated on current track layers. SEM micrographs of 3 track layers sintered at different temperatures are shown in Figure 6. Top view SEM images are shown before and after the aging at 200°C for 100h and for 500h. The microstructure is unchanged. Grain boundaries have not moved during aging, meaning that sintered silver track layers are stable at 200°C during at least 500h.

Moreover, the electrical conductivity of the proposed assemblies has been investigated as a function of the aging time. Results are presented in Figure 7. As for microstructure observations, no significant change can be observed after 1000 h of aging.

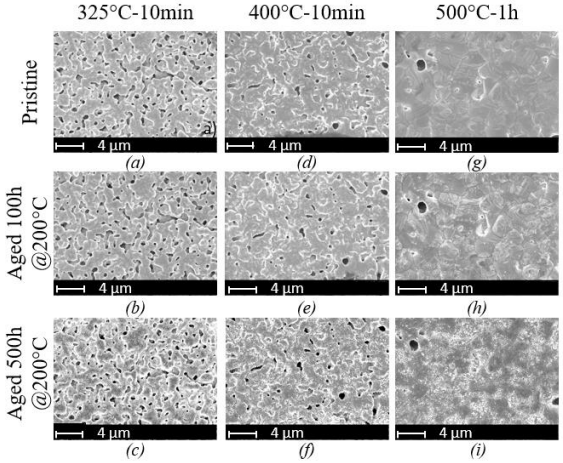

Figure 6: SEM of silver sintered at various conditions before aging (a), (d) and (g), aged at 200°C during 100h (b), (e) and h) and aged at 200°C during 500h (c), (f) and (i).

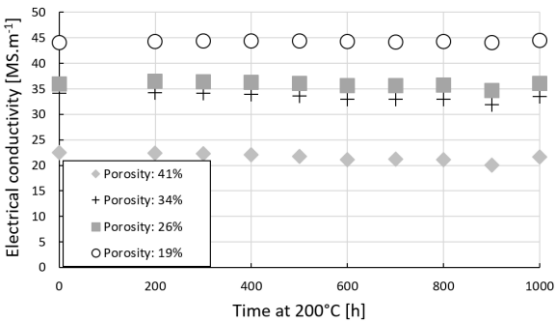

Figure 7: Electrical conductivity vs. aging time at 200°C.

Unlike the microstructure stability observed for current tracks, SEM observations show the

coarsening of the silver microstructure under the device during aging at 200°C in air. Grain size increased significantly during the first 200 h of aging while a slight variation is observed after this time until 500 h (Figure 8a, 8b and 8c). In order to accurately evaluate the microstructure evolution and prevent smearing and smudging of pores during metallographic preparation, cross sections obtained by FIB etching have been observed by SEM for unaged and aged die attach layer sintered at 325°C for 10 min (Figure 8d and 8e). The difference of grain size has been quantified thanks to intercept length measurement. This method consists in measuring the distribution of length of segments crossing the grains on each line of pixels. The distribution density of intercepts is plotted and presented in Figure 8f. The average intercept length increased from 2 µm to 3.9 µm after aging at 200°C and thus confirmed that silver grains in the sintered die attach layer are coarsening during the first 200 h of aging at 200°C in air.

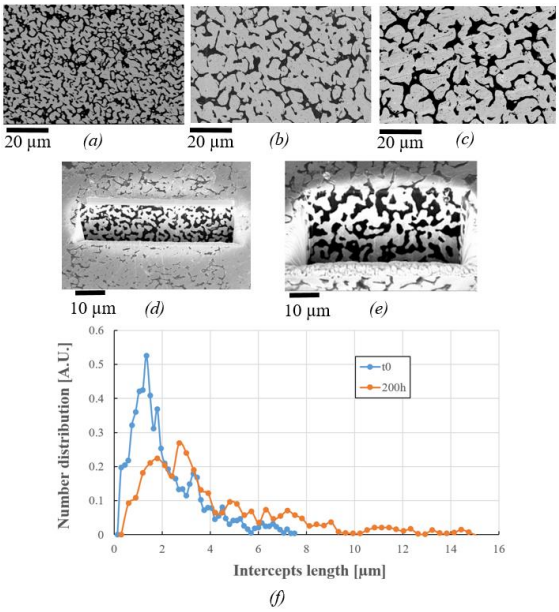

Figure 8: Cross section of silver under die, sintered at 325°C for 10min: unaged (a), aged at 200°C during 200h (b), aged at 200°C during 500h (c), FIB cross section of sample: unaged (d), aged at 200°C during 200h (e), Intercept length distribution of unaged and aged silver at 200°C (f).

Coarsening of sintered silver grains during aging has been previously observed [10][11] but at temperatures higher than the sintering temperature and for aging times much larger than the sintering time. *Chen et al.* have shown that during aging at 250°C in air, a microstructure coarsening took place while the microstructure was stable as the samples were aged in vacuum for the same duration [14]. The authors suggest a possible mechanism of coarsening based on Ag-O complex reactions that can lead to the formation of Ag nanoparticles around micro-particles. But the effect of these nanoparticles on microstructural coarsening is not clear. In this work, the aging temperature is much smaller than the sintering temperature and no microstructural change is observed during aging for the track layer (without chip), as expected, whereas microstructural coarsening occurs in the die attach layer (with chip). In fact, the CTE mismatch between silver joint (20 ppm/°C) and the silicon chip (2.6 ppm/°C) generates tensile stresses inside the silver layer when the temperature of the assembly is below the sintering temperature. Microstructural coarsening is then probably a complex effect of atmosphere, temperature and stresses induced by the thermal process.

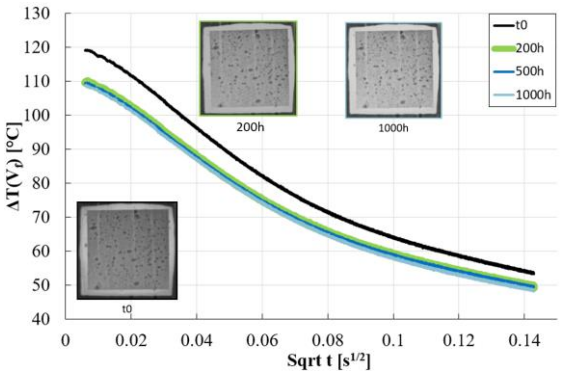

Figure 9: Evolution of the transient thermal response of one diode during aging at 200°C, X-Ray images of sintered silver below the diode for different aging times.

The transient thermal responses of 4 diodes have been studied as a function of the aging time at 200°C in air. The temperature estimated for one diode during cooling as a function of the square root of time after the injection of 120 A during 30 ms can be seen in Figure 9 for several aging durations. In the curves, the data for the shorter times have been hidden because of electrical transient effects which distorted the indirect thermal measurement. The maximal temperature increase has been reduced from 120°C to 110°C after 200 h at 200°C. For longer aging times, the thermal response remained unchanged. The same behavior has been observed for all diodes. The decrease of the maximum temperature between unaged and aged samples suggests an evolution of the structure of the assembly. X-Ray analysis have been achieved in order to check a possible modification of the die attach macrostructure during thermal storage. X-ray radiographic and images are presented at initial time, after 200 h at 200°C and after 1000 h at 200°C in Figure 9. The grey level corresponds to a gradient of matter while black areas correspond to macrovoids. The macrostructures did not change after 1000 h at

200°C. Hence, the evolution of the thermal response must be related to the coarsening of the microstructure of the sintered die attach layer as previously discussed in Figure 8.

Finally, the shear stress tests were performed on samples consisting of 3 layers. Two sintering temperatures of the track layer were tested. The samples were aged at 200°C under air for 200h, 500h and 1000h. The results of the shear stress tests are presented in Figure 10 and show an increase in the shear stress of the samples after 200h of aging in air, followed by a quasi-stabilization until the end of aging tests. The results are similar for the two sintering temperatures of the track layer. The dispersion is higher for the samples with a track layer sintered at 400°C for 10 min.

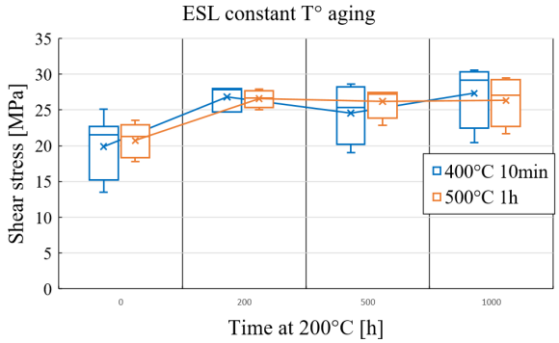

Figure 10: Shear strength as a function of aging time at 200°C for track layers sintered in two conditions.

Optical microscopy measurements of the fractured surfaces showed where the failures occurred. In more than 80% of the cases, the fractures of aged and unaged samples take place at the interfaces of the die attach with the device and with the track layer. As an example, the fracture surface on samples where the track layer was sintered at 500°C during 1h and the die attach layer was sintered at 325°C for 10 min is presented. Figure 11a and 11b present the substrate side for unaged and 1000 h aged samples respectively. Figure 11c and 11d respectively present the die side after 1000 h of aging and the linear profile extracted at the blue lines on the substrate side. It is obvious that before and after 1000h of aging, the steps between the two levels where the failure occurs are about 110µm (±5µm). This value corresponds to the die attach thickness. These analyses confirm that the weakest point of the assembly is the interfaces of the die attach silver sintered material.

Analyses of the fracture surfaces explain the results of shear stress in Figure 10. The fracture takes place at the level of the attach layer. Therefore, a modification of the sintering temperature of the track layer should not impact the shear strength for sintering temperatures of 400°C and 500°C. On the other hand, since the failure occurs in the die attach layer, a change in its microstructure during the aging should have an impact on the shear stress values. This is consistent with the microstructure coarsening of the silver under the chip observed after 200 h of aging. The improvement of shear stress values can be explained by the porosity decreases in the sintered layers or the improvement of the interface adhesion between the die attach layer and the device and/or the track layer during aging.

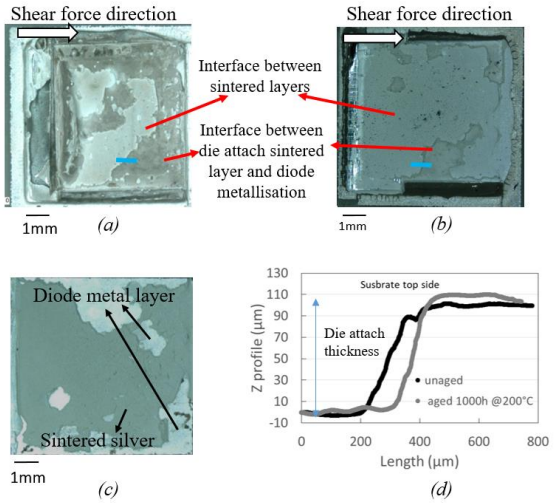

Figure 11: Fracture face seen with optical microscope after shear tests, (a) substrate side of unaged sample, (b) substrate side after 1000 h at 200°C, (c) diode side after 1000 h at 200°C, and (d) profile of the fracture extracted from optical measurement performed at blue lines indicated on the substrate surface in (a) and (b).

4. Conclusions

In order to manufacture power modules able to operate at high temperatures (200°C), an innovative assembly based on multilayers silver sintering to join the electronic devices to AlN ceramic heat sink has been evaluated. The relationship between the process, the microstructure and the physical properties of sintered silver such as porosity, shear resistance, thermal and electrical conductivities have been established. This data will allow to design power modules with the desired specifications. Electrical, thermal and mechanical characterizations after thermal aging for 1000h at 200°C in air showed the suitability of the assembly for high temperature applications.

However, according to the state of the art and the presented results on the microstructure evolution of sintered silver joints during thermal aging at high temperature, it seems that both the oxygen presence and the mechanical stresses in the joint are responsible for microstructure coarsening. Hence, two main factors should be carefully considered for real applications:

1) The presence of the encapsulation material and how it fills the porosity, to reduce the local oxygen partial pressure.

2) The possible presence, the nature and the thickness of the attached materials that can have a significant impact on the stress distribution in the sintered layer (semiconductor material, connector, substrate, heat spreader…).

References

[1] Kyung-ah S et al. GaN-based high temperature and radiation-hard electronics for harsh environments. Nanoscience and Nanotechnology Letters, Vol. 2, No. 2, (2010).

[2] Funaki T et al. SiC JFET dc characteristics under extremely high ambient temperatures. IEICE Electronic Express, Vol. 1, No. 17, (2004).

[3] Ning P et al. IEEE Transactions on Power Electronics, Vol. 25, No. 1, (2010).

[4] Johnson W et al. Packaging of electronics for extreme environment applications. International Planetary Probe workshop, Bordeaux (2007).

[5] Fukumoto A et al. Effects of extreme temperature swings (−55 °C to 250 °C) on silicon nitride active metal brazing substrates. IEEE Trans. Device Mater. Rel., Vol. 14, No. 2, (2014), pp. 751–756.

[6] Rusche et al. Lifetime Analysis of PrimePACK™ Modules with IGBT5 and XT. Bodo's power, (2016).

[7] Khazaka R et al. Survey of High-Temperature Reliability of Power Electronics Packaging Components. IEEE Transaction on power electronics. Vol. 30, No. 5, (2015).

[8] Due J. Reliability of thermal interface materials: A review. Applied Thermal Engineering, Vol. 50, (2013), pp. 455-463.

[9] Khazaka R et al. Review on Joint Shear Strength of Nano-Silver Paste and Its Long-Term High Temperature Reliability. Journal of electronic materials, Vol. 43, No. 7, (2014), pp2459-2466.

[10] Zhang H, et al. Failure analysis and reliability evaluation of silver-sintered die attachment for high-temperature applications. Microelectronics Reliability, Vol. 94, (2019), pp 46–55

[11] Yu F et al. Pressureless Sintering of Microscale Silver Paste for 300 °C Applications. IEEE Transactions on Components, Packaging, and Manufacturing Technology, Vol. 5, No. 9, (2015), pp 1258-1264.

[12] Botter N. et al. (2020). Sintering Behaviour of Silver Paste for Assembly of Power Electronics Components. Euro PM2020 Proceedings. European Powder Metallurgy Association (EPMA).

[13] Siow K. Die-Attach Materials for High Temperature Applications in Microelectronics Packaging. Springer, (2019).

[14] Chuatong C. et al. Effect of oxygen on microstructural coarsening behaviors and mechanical properties of Ag sinter paste during high-temperature storage from macro to micro, Vol 834, (2020), 155173